Johann Radon Institute for
Computational and Applied Mathematics
Austrian Academy of Sciences (ÖAW)

# A multilevel method for discontinuous Galerkin approximation of three-dimensional anisotropic elliptic problems

J. Kraus, S. Tomar

RICAM-Report 2006-39

# A MULTILEVEL METHOD FOR DISCONTINUOUS GALERKIN APPROXIMATION OF THREE-DIMENSIONAL ANISOTROPIC ELLIPTIC PROBLEMS

JOHANNES KRAUS AND SATYENDRA TOMAR

ABSTRACT. We construct optimal order multilevel preconditioners for interior-penalty discontinuous Galerkin (DG) finite element discretizations of three-dimensional (3D) anisotropic elliptic boundary-value problems. In this paper we extend the analysis of our approach, introduced earlier for 2D problems [20], to cover 3D problems. A specific assembling process is proposed which allows us to characterize the hierarchical splitting locally. This is also the key for a local analysis of the angle between the resulting subspaces. Applying the corresponding two-level basis transformation recursively, a sequence of algebraic problems is generated. These discrete problems can be associated with coarse versions of DG approximations (of the solution to the original variational problem) on a hierarchy of geometrically nested meshes. A new bound for the constant $\gamma$ in the strengthened Cauchy-Bunyakowski-Schwarz inequality is derived. The presented numerical results support the theoretical analysis and demonstrate the potential of this approach.

## 1. INTRODUCTION

Discontinuous Galerkin (DG) finite element (FE) methods for elliptic and parabolic problems, though initially proposed in 70s-80s, see [1, 14, 28], have gained much interest in the last decade due to their suitability for *hp*-adaptive techniques. Their application spans a wide variety of problems, see the review article [12] and the references therein. They offer several advantages, e.g. the ease of treatment of meshes with hanging nodes, elements of varying shape and size, polynomials of variable degree, parallelization, preservation of local conservation properties, etc. An excellent overview and a detailed analysis of DG methods for elliptic problems can be found in [2, 11]. Unfortunately, DG discretizations result in excessive number of degrees of freedom (DOF) as compared to their counter-part, i.e. the standard FE methods. Developing efficient preconditioning techniques, which yield fast iterative solvers, thus becomes of significant importance.

Optimal-order preconditioners obtained from recursive application of two-level FE methods have been introduced and extensively analyzed in the context of conforming methods, see e.g., [3, 4, 5, 6]. More recently, some extensions related to Crouzeix-Raviart or Rannacher-Turek nonconforming finite elements have also been considered [9, 16]. For this kind of discretization schemes the finite element spaces corresponding to two successive levels of mesh refinement are not nested in general.

For DG discretizations geometric multigrid (MG) type preconditioners and solvers for the linear system of equations have been considered in [10, 17, 18]. However, our approach on this topic falls within the framework of algebraic multilevel techniques. In [20] we proposed an optimal-order preconditioner for interior penalty (IP) discontinuous Galerkin finite element discretization of 2D isotropic elliptic problems. In this paper we study this

*Key words and phrases.* Discontinuous Galerkin FEM; multilevel preconditioning; hierarchical basis; CBS constant; anisotropic problems.

method for 3D anisotropic problems. The method is obtained from recursive application of the two-level algorithm. A sequence of FE spaces is created using geometrically nested meshes. A specific splitting of the bilinear terms is proposed which results in an assembling process similar to that of the conforming methods. In this approach one avoids the projection onto a coarse (auxiliary) space [13, 21, 22], where the auxiliary space is related to a standard Galerkin discretization, and instead, generates a sequence of algebraic problems associated with a hierarchy of coarse versions of DG approximations of the original problem.

We consider several model problems which range from a simple Poisson problem to a more general and difficult problem with anisotropy alongwith a jump in the coefficients. We present the local analysis of the hierarchical splitting and derive a new bound for the constant $\gamma$ in the strengthened Cauchy-Bunyakowski-Schwarz inequality.

The content of this paper is summarized as follows. In Section 2 we state our model problems. The DG approximation is presented in Section 3, which covers tessellation, function spaces, trace operators and the bilinear form. Discrete formulation and matrix assembly, based on the splitting proposed in [20], are parts of Section 4. In Section 5 the two- and multi-level preconditioning framework is described on the background of a proper hierarchical basis transformation for the linear systems arising from DG discretization. The analysis of the angle between the induced subspaces is the subject of the Section 6. Finally, various numerical experiments are presented in Section 7 and conclusions are drawn in Section 8.

## 2. Model problem

Consider a second order elliptic problem on a bounded Lipschitz domain $\Omega \subset \mathbb{R}^3$:

$$-\nabla \cdot (\underline{A}(x)\nabla u) = \underline{f}(x) \qquad \text{in } \Omega, \tag{1a}$$

$$u(x) = u_D \qquad \text{on } \Gamma_D, \tag{1b}$$

$$\underline{A}\nabla u \cdot \mathbf{n} = u_N \qquad \text{on } \Gamma_N. \tag{1c}$$

Here $\mathbf{n}$ is the exterior unit normal vector to $\partial\Omega \equiv \Gamma$. The boundary is assumed to be decomposed into two disjoint parts $\Gamma_D$ and $\Gamma_N$, and the boundary data $u_D$, $u_N$ are smooth. For the DG formulation below we shall need the existence of the traces of $u$ and $\underline{A}\nabla u \cdot \mathbf{n}$ on the faces in $\Omega$, and the solution $u$ is assumed to have the required regularity. It is assumed that $\underline{A}$ is a symmetric positive definite matrix such that

$$c_1 |\xi|^2 \le \underline{A}\xi \cdot \xi \le c_2 |\xi|^2 \qquad \forall \xi \in \mathbb{R}^3.$$

With $\Omega$ as a unit cube $(0,1)\times(0,1)\times(0,1)$ we shall consider the following cases of the model problem 1 in our analysis and numerical examples:

**Poisson problem::** Consider $\underline{A} = I$, the identity matrix.

**Problem $P_0$::** The coefficient $\underline{A}$ has jumps as follows:

$$\underline{A} = \left\{ \begin{array}{cc} 1 & \text{in } (I_1\times I_1\times I_1)\bigcup(I_2\times I_2\times I_1)\bigcup(I_2\times I_1\times I_2)\bigcup(I_1\times I_2\times I_2) \\ \varepsilon & \text{elsewhere} \end{array} \right\},$$

where $I_1 = (0, 0.5]$ and $I_2 = (0.5, 1)$, and $\varepsilon = \{0.1, 0.01, 0.001\}$.

**Problem $P_1$::** The coefficient $\underline{A}$ has the anisotropy in the $x$ direction as follows:

$$\underline{A} = \left[ \begin{array}{ccc} \mu_x & 0 & 0 \\ 0 & 1 & 0 \\ 0 & 0 & 1 \end{array} \right],$$

where $\mu_x = \{0.1, 0.01, 0.001\}$.

**Problem $P_2$::** The coefficient $\underline{A}$ has the anisotropy in both the directions $x$ and $y$ as follows:

$$\underline{A} = \begin{bmatrix} 0.001 & 0 & 0 \\ 0 & \mu_y & 0 \\ 0 & 0 & 1 \end{bmatrix},$$

where $\mu_y = \{0.1, 0.01, 0.001\}$.

**Problem $P_3$::** The coefficient $\underline{A}$ has the anisotropy in both the directions $x$ and $y$ as well as the jump in the coefficients as follows:

$$\underline{A} = a_\varepsilon \begin{bmatrix} 0.01 & 0 & 0 \\ 0 & 0.1 & 0 \\ 0 & 0 & 1 \end{bmatrix},$$

where

$$a_\varepsilon = \left\{ \begin{array}{cc} 1 & \text{in } (I_1 \times I_1 \times I_1) \bigcup (I_2 \times I_2 \times I_1) \bigcup (I_2 \times I_1 \times I_2) \bigcup (I_1 \times I_2 \times I_2) \\ \varepsilon & \text{elsewhere} \end{array} \right\},$$

and $\varepsilon = \{0.1, 0.01, 0.001\}$.

Note that without any loss of generality we can assume that the coefficient $\underline{A}$ is normalized with respect to the diffusion in the $z$ direction.

## 3. DG approximation

Let $\mathcal{T}_h$ be a non-overlapping partition of $\Omega$ into a finite number of elements $e$. For any $e \in \mathcal{T}_h$ we denote its diameter by $h_e$ and the boundary by $\partial e$. Let $f = \bar{e}^+ \cap \bar{e}^-$ be a common face of two adjacent elements $e^+$, and $e^-$. Further, let $h = \max_{e \in \mathcal{T}_h} h_e$ denotes a characteristic mesh size of the whole partition. The set of all the internal faces is denoted by $\mathcal{F}_0$, and $\mathcal{F}_D$ and $\mathcal{F}_N$ contain the faces of finite elements that belong to $\Gamma_D$ and $\Gamma_N$, respectively. Finally, $\mathcal{F}$ is the set of all the faces, i.e., $\mathcal{F} = \mathcal{F}_0 \cup \mathcal{F}_D \cup \mathcal{F}_N$. We assume that the partition is shape-regular, see [26]. We allow finite elements to vary in size and shape for local mesh adaptation and the mesh is not required to be conforming, i.e. elements may possess hanging nodes. Further, the face measure $h_f$ is a quantity defined on each face $f \in \mathcal{F}$ as follows

$$h_f = |f|^{\frac{1}{2}}, \quad \text{for } f \in \mathcal{F}.$$

On the partition $\mathcal{T}_h$ we define a broken Sobolev space:

$$\mathcal{V} := H^2(\mathcal{T}_h) = \{v \in L^2(\Omega) : v|_e \in H^2(e), \forall e \in \mathcal{T}_h\}.$$

Note that the functions in $\mathcal{V}$ **may not satisfy** any boundary condition. By

$$\mathcal{V}_h := \mathcal{V}_h(\mathcal{T}_h) = \{v \in L^2(\Omega) : v|_e \in P_r(e), \forall e \in \mathcal{T}_h\},$$

where $P_r$ is the set of polynomials of degree $r \geq 1$, we define a finite dimensional subspace of $\mathcal{V}$. Obviously, $\mathcal{V}_h = \Pi_{e \in \mathcal{T}_h} P_r(e)$. Further, for the vector-valued functions we define the following spaces:

$$\mathcal{Q} := \left(H^2(\mathcal{T}_h)\right)^3 = \{\mathbf{q} \in \left(L^2(\Omega)\right)^3 : \mathbf{q}|_e \in \left(H^2(e)\right)^3, \forall e \in \mathcal{T}_h\},$$

$$\mathcal{Q}_h := \mathcal{Q}_h(\mathcal{T}_h) = \{\mathbf{q} \in \left(L^2(\Omega)\right)^3 : \mathbf{q}|_e \in (P_r(e))^3, \forall e \in \mathcal{T}_h\}.$$

For ease of the notations in what follows, on $\mathcal{V}$ we introduce the following forms

$$(\underline{A}\nabla_h u_h, \nabla_h v_h)_{\mathcal{T}_h} := \sum_{e \in \mathcal{T}_h} \int_e \underline{A}\nabla_h u_h \cdot \nabla_h v_h dx, \quad \langle p, q \rangle_{\mathcal{F}^g} := \sum_{f \in \mathcal{F}^g} \int_f p \cdot q ds,$$

where $\mathcal{F}^g$ is one of the sets $\mathcal{F}$, $\mathcal{F}_0$, $\mathcal{F}_D$, $\mathcal{F}_N$ or their combinations.

To deal with multivalued traces at the element faces in a DG discretization we introduce some trace operators. We define the *average* ($\{\cdot\}$) and *jump* ($[\![\cdot]\!]$) as follows:
Let $f$ be an interior face shared by elements $e^+$ and $e^-$. Define the unit normal vectors $\mathbf{n}^+$ and $\mathbf{n}^-$ on $f$ pointing exterior to $e^+$ and $e^-$, respectively. For $v \in \mathcal{V}$ we define $v^{+/-} := v|_{\partial e^{+/-}}$ and set

$$\{v\} = \frac{1}{2}\left(v^+ + v^-\right), \qquad [\![v]\!] = v^+\mathbf{n}^+ + v^-\mathbf{n}^- \quad \text{on } f \in \mathcal{F}_0.$$

For a piece-wise smooth vector-valued function $\mathbf{q} \in Q$ the definitions are similar and we set

$$\{\mathbf{q}\} = \frac{1}{2}\left(\mathbf{q}^+ + \mathbf{q}^-\right), \qquad [\![\mathbf{q}]\!] = \mathbf{q}^+ \cdot \mathbf{n}^+ + \mathbf{q}^- \cdot \mathbf{n}^- \quad \text{on } f \in \mathcal{F}_0.$$

On $f \in \mathcal{F}_D \cup \mathcal{F}_N$ the functions $v$ and $\mathbf{q}$ are uniquely defined and we only require $[\![v]\!]$ and $\{\mathbf{q}\}$, which are set as

$$[\![v]\!] = v\mathbf{n}, \qquad \{\mathbf{q}\} = \mathbf{q}.$$

Finally, on $\mathcal{V}$ we define the following mesh-dependent broken norm:

$$|\![v_h]\!|^2 = (\underline{A}\nabla_h v_h, \nabla_h v_h)_{\mathcal{T}_h} + \alpha h_f^{-1} \langle [\![v_h]\!], [\![v_h]\!] \rangle_{\mathcal{F}_0 \cup \mathcal{F}_D}. \tag{2}$$

Let us now recall the DG formulation for second order elliptic problems. In recent years a large number of DG FEM were developed for elliptic boundary value problems, for review see, e.g. [2, 11] and the references therein. Below, we consider the standard interior penalty (IP) DG method, see, e.g., [1, 2]. For the problem (1), the primal IP-DG formulation can be stated as follows:
Find $u_h \in \mathcal{V}$ such that

$$\mathcal{A}(u_h, v_h) = \mathcal{L}(v_h), \quad \forall v_h \in \mathcal{V}, \tag{3a}$$

where the bilinear form $\mathcal{A}(\cdot,\cdot) : \mathcal{V} \times \mathcal{V} \to \mathbb{R}$ and the linear form $\mathcal{L}(\cdot) : \mathcal{V} \to \mathbb{R}$ are defined by the relations

$$\begin{aligned} \mathcal{A}(u_h, v_h) =& (\underline{A}\nabla_h u_h, \nabla_h v_h)_{\mathcal{T}_h} + \alpha h_f^{-1} \langle [\![u_h]\!], [\![v_h]\!] \rangle_{\mathcal{F}_0 \cup \mathcal{F}_D} \\ & - \langle \{\underline{A}\nabla_h u_h\}, [\![v_h]\!] \rangle_{\mathcal{F}_0 \cup \mathcal{F}_D} - \langle [\![u_h]\!], \{\underline{A}\nabla_h v_h\} \rangle_{\mathcal{F}_0 \cup \mathcal{F}_D}, \end{aligned} \tag{3b}$$

$$\mathcal{L}(v_h) = \int_\Omega f v_h dx + \alpha h_f^{-1} \langle u_D, v_h \rangle_{\mathcal{F}_D} - \langle u_D \mathbf{n}, \underline{A}\nabla_h v_h \rangle_{\mathcal{F}_D} + \langle g_N, v_h \rangle_{\mathcal{F}_N}. \tag{3c}$$

Here $\alpha$ is a parameter which is to be defined to guarantee the coercivity of the bilinear form $\mathcal{A}$.

As usual, we assume that the Dirichlet boundary conditions are defined by a given function $u_D \in H^1(\Omega)$ in the sense that the trace of $u - u_D$ on $\Gamma_D$ is zero. For the sake of simplicity, we also assume that $u_D$ is such that the boundary condition can be exactly satisfied by the approximations used.

It can be proved (see, e.g., [2]) that the bilinear form $\mathcal{A}$ is coercive and bounded on $\mathcal{V}$ equipped with the norm (2) provided that $\alpha > 0$ is sufficiently large. Recently, a lower bound and explicit expression for $\alpha$ to guarantee the coercivity was obtained in [27]. Moreover, it is well known that for $f \in L^2(\Omega)$ the problem (3a) is well-posed and possesses a unique solution $u_h \in \mathcal{V}$. Assume that $u \in H^s(\Omega)$, $2 \le s \le r+1$. Then, an optimal order of convergence, given by the following estimates, can be obtained in both the norms $|\![\cdot]\!|$ and $\|\cdot\|$

$$\begin{aligned} |\![u - u_h]\!| &\le C h^{s-1} \|u\|_{H^s(\Omega)}, \\ \|u - u_h\|_{L^2(\Omega)} &\le C h^s \|u\|_{H^s(\Omega)}. \end{aligned}$$

For the proof we refer to [2].

## 4. Discrete formulation and matrix assembly

The weak formulation (3) is transformed into a set of algebraic equations by approximating $u_h$ and $v_h$ using linear polynomials in each element as

$$u_{e,h} = \sum_{j=0}^{7} \widetilde{u}_{e,j} \mathcal{N}_{e,j}(x), \quad v_{e,h} = \sum_{j=0}^{7} \widetilde{v}_{e,j} \mathcal{N}_{e,j}(x), \quad x \in e \subset \mathbb{R}^3. \tag{4}$$

Here $\widetilde{u}_{e,j} \in \mathbb{R}^8$ and $\widetilde{v}_{e,j} \in \mathbb{R}^8$ are the expansion coefficients of $u_h$ and the test function $v_h$ in the element $e$, respectively, and $\mathcal{N}_{e,j}$ are the trilinear basis functions.

We now briefly show the computation of the element stiffness matrix. Consider a general element $e$ with all its face internal. Let its neighboring elements, which share a face with this element, be denoted by $e_1^+$, $e_2^+$, $e_3^+$, $e_4^+$, $e_5^+$, and $e_6^+$. Here $\cdot^+$ represents the neighboring element and digits $1, \ldots, 6$ represent the face number with which the neighboring element is attached. This arrangement is depicted in Figure 1. Note that the occurence of each degree of freedom (DOF) thrice is only to depict that it is common to three faces. Using the definition of the trace operators $\{\cdot\}$ and $[\![\cdot]\!]$ and the specific splitting of the bilinear terms proposed in [20] the resulting elemental bilinear form reads

$$\begin{aligned} \mathcal{A}_e(u_h, v_h) = & \int_e \underline{A} \nabla_h u_h \cdot \nabla_h v_h dx - \frac{1}{2} \sum_{s=1}^{6} \int_{f_s} \Big( \big( v_e \mathbf{n}_e + v_{e_s^+} \mathbf{n}_{e_s^+} \big) \cdot \underline{A} \nabla_h u_e \\ & + \underline{A} \nabla_h v_e \cdot \big( u_e \mathbf{n}_e + u_{e_s^+} \mathbf{n}_{e_s^+} \big) \Big) ds \\ & + \frac{\alpha h_f^{-1}}{2} \sum_{s=1}^{6} \int_{f_s} \big( v_e \mathbf{n}_e + v_{e_s^+} \mathbf{n}_{e_s^+} \big) \cdot \big( u_e \mathbf{n}_e + u_{e_s^+} \mathbf{n}_{e_s^+} \big) ds. \end{aligned} \tag{5}$$

In this approach, as depicted in Figure 1, the DOF of the element $e$ are connected with only those DOF of its neighboring elements $e_s^+$ which are at the common face. The size of the elemental stiffness matrix $A_e$ is $32 \times 32$ and the details are provided in the Appendix.

Now let $N = 8N_e$ denote the total number of DOF in the system. Using the polynomial approximation (4) into the weak form (3), with elemental bilinear form (5), we get the following linear system of equations

$$A\mathbf{x} = \mathbf{b}, \tag{6}$$

where $\mathbf{x} \in \mathbb{R}^N$, $A \in \mathbb{R}^{N \times N}$ with $N_e^2$ blocks of size $8 \times 8$, and $\mathbf{b} \in \mathbb{R}^N$, denote the vector of expansion coefficients, the global stiffness matrix, and the right hand side data vector, respectively.

## 5. Multilevel preconditioning using hierarchical basis

In this section we will define the two-level hierarchical basis (HB) transformation which we shall use in the construction of the multilevel preconditioner. This transformation, when applied recursively, relates to a sequence of hierarchical meshes, which in our case generate a nested sequence of finite element spaces.

Let us consider a hierarchy of partitions $\mathcal{T}_{h_\ell} \subset \mathcal{T}_{h_{\ell-1}} \subset \ldots \subset \mathcal{T}_{h_1} \subset \mathcal{T}_{h_0}$ of $\Omega$, where the notation $\mathcal{T}_{h_k} = \mathcal{T}_h \subset \mathcal{T}_H = \mathcal{T}_{h_{k-1}}$ points out the fact that for any element $e$ of the fine(r) partition $\mathcal{T}_h$ there is an element $E$ of the coarse(r) mesh partition $\mathcal{T}_H$ such that $e \subset E$. For the construction of the preconditioner of the linear system (6) resulting from the IP-DG approximation of the basic problem (1) its DOF are partitioned into a *fine* and a *coarse* (sub-) set, indicated by the subscripts 1 and 2, respectively. The partitioning is induced by a regular mesh refinement at every level $(k-1) = 0, 1, \ldots, \ell - 1$. In other words, by halving

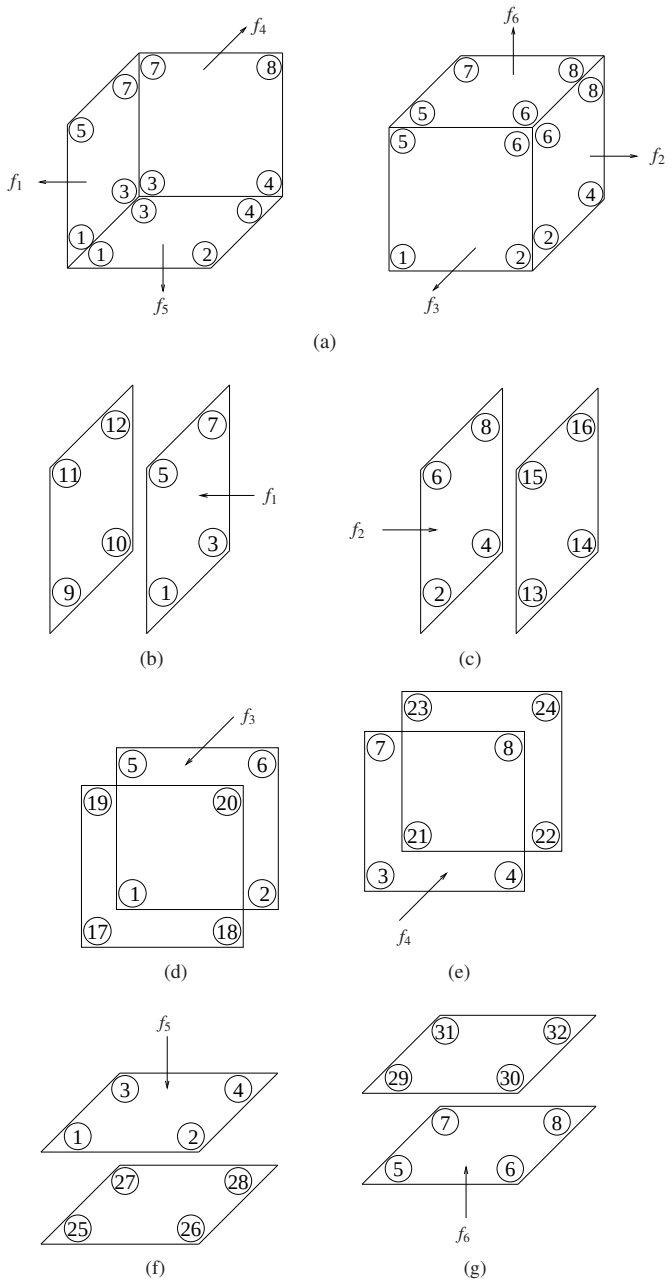


FIGURE 1. Specific arrangement of elemental DOF

the meshsize, i.e., $h = H/2$, each element is subdivided into eight elements of similar shape, herewith producing the mesh at levels $k = 1, 2, \ldots, \ell$. Hence, the linear system (6)

can be represented in the $2 \times 2$ block form as

$$\begin{bmatrix} A_{11} & A_{12} \\ A_{21} & A_{22} \end{bmatrix} \begin{pmatrix} \mathbf{x}_1 \\ \mathbf{x}_2 \end{pmatrix} = \begin{pmatrix} \mathbf{b}_1 \\ \mathbf{b}_2 \end{pmatrix} \tag{7}$$

where $A_{21} = A_{12}^T$. By using the two-level transformation matrix

$$J = \begin{bmatrix} I_{11} & P_{12} \\ 0 & I_{22} \end{bmatrix}, \tag{8}$$

the system to be solved in the hierarchical basis has the representation

$$\widehat{A}\,\widehat{\mathbf{x}} = \widehat{\mathbf{b}}, \tag{9}$$

where $\widehat{A}$ and its submatrices $\widehat{A}_{11}, \widehat{A}_{12}\ \widehat{A}_{21}, \widehat{A}_{22}$ are given by

$$\widehat{A} = J^T A\, J = \begin{bmatrix} \widehat{A}_{11} & \widehat{A}_{12} \\ \widehat{A}_{21} & \widehat{A}_{22} \end{bmatrix}, \tag{10a}$$

$$\widehat{A}_{11} = A_{11}, \quad \widehat{A}_{12} = A_{11}P_{12} + A_{12}, \quad \widehat{A}_{21} = P_{12}^T A_{11} + A_{21}, \tag{10b}$$

$$\widehat{A}_{22} = P_{12}^T A_{11} P_{12} + A_{21} P_{12} + P_{12}^T A_{12} + A_{22}. \tag{10c}$$

The vectors $\widehat{\mathbf{x}}$ and $\widehat{\mathbf{b}}$ are transformed then from hierarchical basis to a nodal basis via $\mathbf{x} = J\widehat{\mathbf{x}}$ and $\widehat{\mathbf{b}} = J^T\mathbf{b}$, and the following relations hold

$$\mathbf{x}_1 = \widehat{\mathbf{x}}_1 + P_{12}\widehat{\mathbf{x}}_2, \quad \mathbf{x}_2 = \widehat{\mathbf{x}}_2, \tag{11a}$$

$$\widehat{\mathbf{b}}_1 = \mathbf{b}_1, \qquad \widehat{\mathbf{b}}_2 = P_{12}^T\mathbf{b}_1 + \mathbf{b}_2. \tag{11b}$$

When constructing the global interpolation matrix $P_{12}$ we aim at achieving that the matrix $\widehat{A}_{22}$, which is associated with the coarser mesh partition, comes out as a coarse(r) version of the same kind of IP-DG discrete problem. In particular, the matrix $\widehat{A}_{22}$ should have a similar sparsity pattern as $A$ and the transformation (10a) should allow for an efficient change of bases. This requires a local support of the interpolation. In addition, we want to be able to characterize the transformation locally. In order to achieve this common purpose we use the same simple interpolation, based on averaging, as has been proposed in [20] for two-dimensional problems.

The general macro element we are using to define the local interpolation $P_E$ is simply the union of eight elements that share one vertex. Based on the element matrices, see the Appendix, the macro element accumulates 160 DOF, 32 of which define then an element on the next coarser level. The interpolation weights are simply taken to be $1/8$ for the 8 interior fine DOF (interpolating from every interior coarse DOF), $1/4$ for the 48 fine DOF located at the center of the faces of the macro-element (interpolating from coarse DOF belonging to the same face), and $1/2$ for the 72 fine DOF associated with macro-element edges (where interpolation again is only from coarse DOF of the same macro-edge). This results in the local macro-element two-level transformation matrix

$$J_E = \begin{bmatrix} I & P_E \\ 0 & I \end{bmatrix}, \tag{12}$$

where the macro-element interpolation matrix $P_E$ is of size $128 \times 32$.[1]

[1]This construction is a straightforward generalization of the transformation Variant 1 in Reference [20].

The construction of the multilevel preconditioner then is as follows: Starting from the coarsest mesh (level 0) with $M^{(0)} = A^{(0)}$, the goal is to apply the (multiplicative) two-level preconditioner $M^{(k)}$ recursively at all levels of mesh refinement:

$$M^{(k)} = \begin{bmatrix} C_{11}^{(k)} & 0 \\ \widehat{A}_{21}^{(k)} & C_{22}^{(k)} \end{bmatrix} \begin{bmatrix} I & C_{11}^{(k)^{-1}} \widehat{A}_{12}^{(k)} \\ 0 & I \end{bmatrix}, \quad k = 1, 2, \ldots, \ell. \tag{13}$$

Here $C_{11}^{(k)}$ is a preconditioner for the upper-left pivot block of the (hierarchical) stiffness matrix

$$\widehat{A}^{(k)} = \begin{bmatrix} \widehat{A}_{11}^{(k)} & \widehat{A}_{12}^{(k)} \\ \widehat{A}_{21}^{(k)} & \widehat{A}_{22}^{(k)} \end{bmatrix},$$

and the matrix $C_{22}^{(k)}$ is implicitly given by the equation

$$C_{22}^{(k)^{-1}} = \left[ I - P_\beta \left( M^{(k-1)^{-1}} \widehat{A}^{(k-1)} \right) \right] \widehat{A}^{(k-1)^{-1}} \tag{14}$$

with $M^{(k-1)}$ and $\widehat{A}^{(k-1)}$ denoting the multiplicative preconditioner and the stiffness matrix at level $(k-1)$, respectively. Moreover, $\widehat{A}^{(0)} = A^{(0)}$ by definition. Then, as well known from theory [5, 6], a properly shifted Chebyshev polynomial $P_\beta$ of degree $\beta$, satisfying the conditions

$$0 \le P_\beta(t) < 1, \quad 0 < t \le 1, \quad P_\beta(0) = 1,$$

can be used to stabilize the condition number. Alternatively, a few inner generalized conjugate gradient (GCG) type iterations are employed in the nonlinear algebraic multilevel iteration (NLAMLI) method. The whole iterative solution process is of optimal computational complexity if the degree $\beta_k = \beta$ of the matrix polynomial (or alternatively, the number of inner iterations at level $k$ for NLAMLI) satisfies the condition

$$1/\sqrt{(1-\gamma^2)} < \beta < \tau, \tag{15}$$

where $\tau \approx N_k/N_{k-1}$ denotes the reduction factor of the number of DOF, and $\gamma$ denotes the constant in the strengthened Cauchy-Bunyakowski-Schwarz (CBS) inequality, cf. Section 6. The exact value of $\tau$ for DG approximations of 3D problems is 8.

## 6. Local estimate of the constant in the Cauchy-Bunyakowski-Schwarz inequality

It is known that the constant $\gamma$ in the Cauchy-Bunyakowski-Schwarz (CBS) inequality, which is associated with the abstract angle between the two subspaces induced by the two-level hierarchical basis transformation, plays a key role in the derivation of optimal convergence rate estimates for two- and multilevel methods. Moreover, the value of the upper bound for $\gamma \in (0,1)$ is part of the construction of a proper stabilization polynomial in the linear algebraic multilevel iteration (LAMLI) method, see [5, 6].

For the constant $\gamma$ in the strengthened CBS inequality, the following relation holds

$$\gamma = \cos(\mathcal{V}_1, \mathcal{V}_2) = \sup_{u \in \mathcal{V}_1,\ v \in \mathcal{V}_2} \frac{\mathcal{A}(u,v)}{\sqrt{\mathcal{A}(u,u)\mathcal{A}(v,v)}}, \tag{16}$$

where $\mathcal{A}(\cdot,\cdot)$ is the bilinear form given by (3b). If $\mathcal{V}_1 \cap \mathcal{V}_2 = \{0\}$ then $\gamma$ is strictly less than one. As shown in [4], the constant $\gamma$ can be estimated locally over each macro-element $E \in \mathcal{T}_H$, i.e. $\gamma \le \max_E \gamma_E$, where

$$\gamma_E = \sup_{u \in \mathcal{V}_1(E),\ v \in \mathcal{V}_2(E)} \frac{\mathcal{A}_E(u,v)}{\sqrt{\mathcal{A}_E(u,u)\mathcal{A}_E(v,v)}}, \quad v \neq \text{const.}$$

The abovementioned spaces $\mathcal{V}_m(E), m = 1, 2$, contain the functions from $\mathcal{V}_m$ restricted to $E$ and $\mathcal{A}_E(u, v)$ corresponds to $\mathcal{A}(u, v)$ restricted to the macro element $E$ (see also [15]).

Evidently, the global two-level stiffness matrix $\widehat{A}$ can be assembled from the macro-element two-level stiffness matrices $\widehat{A}_E$, which are obtained from assembling the element matrices for all elements $e$ contained in $E$ in the (local) hierarchical basis. In simplified notation this can be written as

$$\widehat{A} = J^T A\, J = \sum_{E\in\mathcal{T}_H} \widehat{A}_E = \sum_{E\in\mathcal{T}_H} J_E^T A_E\, J_E.$$

Like the global matrix, the local matrices are also of the following $2 \times 2$ block form

$$\widehat{A}_E = \begin{bmatrix} \widehat{A}_{E,11} & \widehat{A}_{E,12} \\ \widehat{A}_{E,21} & \widehat{A}_{E,22} \end{bmatrix} = J_E^T \begin{bmatrix} A_{E,11} & A_{E,12} \\ A_{E,21} & A_{E,22} \end{bmatrix} J_E, \tag{17}$$

where $J_E$ is defined by (12) and the transformation-invariant (local) Schur complement is given by

$$S_E = \widehat{A}_{E,22} - \widehat{A}_{E,21}\widehat{A}_{E,11}^{-1}\widehat{A}_{E,12} = A_{E,22} - A_{E,21}A_{E,11}^{-1}A_{E,12}. \tag{18}$$

We know from the general framework of two-level block (incomplete) factorization methods that it suffices to compute the minimal eigenvalue $\lambda_{E;\min}$ of the generalized eigenproblem

$$S_E \mathbf{v}_{E,2} = \lambda_E \widehat{A}_{E,22}\mathbf{v}_{E,2}, \quad \mathbf{v}_{E,2} \perp (1, 1, \ldots, 1)^T, \tag{19}$$

in order to conclude the following upper bound for the constant $\gamma$ in (16):

$$\gamma^2 \le \max_{E\in\mathcal{T}_H} \gamma_E^2 = \max_{E\in\mathcal{T}_H}(1 - \lambda_{E;\min}). \tag{20}$$

This relation then implies condition number estimates for the corresponding two-level preconditioner (of additive and multiplicative type), see, e.g., [3].

The analysis of multilevel methods obtained by recursive application of the two-level preconditioner necessitates the establishment of this kind of (local) bounds for each coarsening step since the two-level hierarchical basis transformation is also applied recursively. This requires the knowledge of the related (macro) element matrices on all coarse levels. For our hierarchical basis transformation, as described in the previous section, we have a very simple recursion relation for the element matrices. This recursion relation shows that the sequence of (global) coarse-grid matrices can be associated with coarse-discretizations of the original problem but with an exponentially increasing sequence of stabilization parameters $\alpha^{(j)}$.

**Lemma 6.1.** *Let $\widehat{A}^{(\ell)} := (J^{(\ell)})^T A\, J^{(\ell)}$ denote the stiffness matrix from (6) in hierarchical basis, where $A = \sum_{e\in\mathcal{T}_h} A_e$ and $A_e = A_e(\alpha) =: A_e^{(0)}(\alpha)\ \forall e \in \mathcal{T}_h$ denotes the element matrix as given in the Appendix. Let us further assume that $A_e$ has the same representation over all the elements of the domain. Then, if one neglects the correction matrices related to the boundary conditions, the coarse-grid problem at level $(\ell - j)$, $j = 1, \ldots, \ell$, (involving the matrices $J^{(\ell)}, J^{(\ell-1)}, \ldots, J^{(\ell-j+1)}$) is characterized by the element matrix*

$$A_e^{(j)}(\alpha) = A_e(\alpha^{(j)}) = A_e(2^j\,\alpha). \tag{21}$$

*In other words, the stabilization parameter $\alpha$ after $j$ applications of the HB transformation equals $\alpha^{(j)} = 2^j\,\alpha$.*

*Proof.* Follows from direct calculation. ∎

**Remark 6.1.** *The assumption of $A_e$ having the same representation over the whole domain can be relaxed to assuming that at least all the fine-grid elements contained in any particular coarse-grid element of the coarsest mesh partition $\mathcal{T}_{h_0}$ have the same element matrix. In this case we allow arbitrary large jumps in the coefficients across the interfaces between adjacent elements of $\mathcal{T}_{h_0}$.*

Due to the explicit representation of the element stiffness matrices, given by Lemma 6.1, the multilevel splitting based on this particular two-level HB transformation is accessible for a local analysis. In the following we prove a lower bound for the minimal eigenvalue of (19). However, since the local macro-element matrix $\widehat{A}_E$ is of size 160×160 with a lower-right block $\widehat{A}_{E,22}$ of size 32×32 a straightforward symbolic solution of (19) is prohibitively complicated (for generic parameters $\alpha$, $\mu_x$, and $\mu_y$). In the proof of the following theorem we will therefore provide the steps for checking the correctness of a lower bound as a function of $\alpha$.

**Theorem 6.1.** *Let $\mu_x = \mu_y = 1$. Consider the HB macro-element matrix $\widehat{A}_E^{(j)}(\alpha)$ associated with the eight elements defining the macro-element as a cube with side $2\,h_{\ell-j}$ where the element matrix $A_e^{(j)}(\alpha)$ from Lemma 6.1 is used in the standard way to assemble $A_E^{(j)}(\alpha)$. Then for the eigenvalues of (19) we have the lower bound*

$$\lambda_{E;\min}^{(j)} = \lambda_{E;\min}(\alpha^{(j)}) \geq \frac{1}{16}\left(1 - \frac{1}{\sqrt{2}\,\alpha^{(j)}}\right) = \frac{1}{16}\left(1 - \frac{1}{\sqrt{2}\,2^j\,\alpha}\right) \quad \forall \alpha \geq 3/2 \tag{22}$$

*and thus*

$$\gamma_E \leq \sqrt{\frac{15}{16} + \frac{1}{16\,\sqrt{2}\,\alpha^{(j)}}} \tag{23}$$

*holds.*

*Proof.* From one of the important properties of the Schur complement $S_E$ in (19), which is related to the minimum energy extension, we know that

$$\mathbf{v}_{E,2}^T S_E \mathbf{v}_{E,2} = \min_{\mathbf{v}_{E,1}} \begin{pmatrix} \mathbf{v}_{E,1} \\ \mathbf{v}_{E,2} \end{pmatrix}^T \begin{bmatrix} A_{E,11} & A_{E,12} \\ A_{E,21} & A_{E,22} \end{bmatrix} \begin{pmatrix} \mathbf{v}_{E,1} \\ \mathbf{v}_{E,2} \end{pmatrix} \quad \forall \mathbf{v}_{E,2}. \tag{24}$$

Thus, if we want to verify any lower bound $\underline{\lambda}$ for the minimal eigenvalue $\lambda_{E;\min}^{(j)}$ of (19), we can rewrite

$$\mathbf{v}_{E,2}^T S_E \mathbf{v}_{E,2} \geq \underline{\lambda}\, \mathbf{v}_{E,2}^T \widehat{A}_{E,22} \mathbf{v}_{E,2} \quad \forall \mathbf{v}_{E,2}$$

in the form

$$\min_{\mathbf{v}_{E,1}} \begin{pmatrix} \mathbf{v}_{E,1} \\ \mathbf{v}_{E,2} \end{pmatrix}^T \begin{bmatrix} A_{E,11} & A_{E,12} \\ A_{E,21} & A_{E,22} - \underline{\lambda}\,\widehat{A}_{E,22} \end{bmatrix} \begin{pmatrix} \mathbf{v}_{E,1} \\ \mathbf{v}_{E,2} \end{pmatrix} \geq 0 \quad \forall \mathbf{v}_{E,2}. \tag{25}$$

Therefore, denoting by $B$ the matrix in (25), i.e.,

$$B := \begin{bmatrix} A_{E,11} & A_{E,12} \\ A_{E,21} & A_{E,22} - \underline{\lambda}\,\widehat{A}_{E,22} \end{bmatrix},$$

it is sufficient to show that $B$ is symmetric positive semidefinite (SPSD) for

$$\underline{\lambda} = \underline{\lambda}(\alpha^{(j)}) := \frac{1}{16}\left(1 - \frac{1}{\sqrt{2}\,\alpha^{(j)}}\right). \tag{26}$$

The particular form of (26) allows us to split the matrix $B$ in the form

$$B \;=\; B_0 + \alpha\, B_1 + \frac{1}{\alpha} B_2 \tag{27}$$

where $\alpha = \alpha^{(j)}$ and the matrices $B_0$, $B_1$, and $B_2$ do not depend on $\alpha$. It turns out that from the matrices $B_k$, $k = 0, 1, 2$, only $B_1$ is SPSD. However, $B_0 + \sqrt{2}\, B_1$ is SPSD as well. We further split $B_2$ then into the sum of an SPSD matrix $B_2^+$ and a symmetric negative semidefinite $B_2^-$ remainder, i.e.,

$$B_2 = B_2^+ + B_2^-. \tag{28}$$

This can easily be done by first transforming $B_2$ into diagonal form, i.e., $V^T B_2 V = D$, then split the diagonal matrix $D$ according to its non-negative and non-positive entries, i.e., $D = D^+ + D^-$, and finally use $B_2^+ := V^{-T} D^+ V^{-1}$ and $B_2^- := V^{-T} D^- V^{-1}$ in (28). We now estimate the quadratic form associated with $B$ by dropping $B_2^+$, i.e.,

$$\mathbf{v}_E^T B \mathbf{v}_E \geq \mathbf{v}_E^T \left( (B_0 + \sqrt{2}\, B_1) + (\alpha - \sqrt{2}) B_1 + \frac{1}{\alpha} B_2^- \right) \mathbf{v}_E =: \mathbf{v}_E^T \underline{B}(\alpha) \mathbf{v}_E \quad \forall \mathbf{v}_E. \tag{29}$$

Since $\mathbf{v}_E^T \underline{B}(\alpha) \mathbf{v}_E$ for any vector $\mathbf{v}_E$ is monotonically increasing in $\alpha$, i.e.,

$$\mathbf{v}_E^T \left( \underline{B}(\alpha) - \underline{B}(\alpha') \right) \mathbf{v}_E \geq 0 \quad \forall \alpha \geq \alpha',$$

and $\underline{B}(\frac{3}{2})$ is SPSD, the lower bound (26) holds true. Together with (20) the estimate (23) is obtained. ∎

**Remark 6.2.** *The bound (23) in Theorem 6.1 tells us that the condition number of the multiplicative preconditioner (with exact inversion of the $A_{11}$-block) can be stabilized using Chebyshev polynomials of degree five. However, as illustrated in the numerical examples below, this goal can also be achieved by employing four inner generalized conjugate gradient iterations.*

## 7. Numerical results

In this section we present numerical results of various examples which aim to validate the analysis and demonstrate the capabilities of the method. The computations are performed on Sun Fire V40z workstation with 4 AMD Opteron 852 CPUs (2.6GHz) with 32 GB RAM. For approximating $u$ in all the examples we use trilinear elements i.e. linear shape functions for each of the variables $x$, $y$, and $z$. The stabilization parameter $\alpha$ is taken as 10. The pivot block in the multilevel preconditioner is approximated using incomplete LU (ILU) factorization based on a drop tolerance tol [20, 25]. The tolerance tol is chosen heuristically by relating it to the parameters $\varepsilon$, $\mu_x$ and $\mu_y$.

**Example 7.1.** *Consider the Poisson problem with homogenous Dirichlet boundary conditions and choose $f$ such that the analytic solution of the problem is given by $u = x(1-x)\, y(1-y)\, z(1-z) \exp(2x + 2y + 2z)$. The tolerance* tol *is taken as* $10^{-2}$.

**Example 7.2.** *Consider Problem $P_0$ with homogenous Dirichlet boundary conditions and $f = 1$. In this example the tolerance* tol *is taken as $\varepsilon \times 10^{-2}$.*

**Example 7.3.** *Consider Problem $P_1$ with homogenous Dirichlet boundary conditions and $f = 1$. In this example the tolerance* tol *is taken as $\mu_x \times 10^{-2}$.*

**Example 7.4.** *Consider Problem $P_2$ with homogenous Dirichlet boundary conditions and $f = 1$. In this example the tolerance* tol *is taken as* $10^{-5}$. *The different treatment of* tol *as compared to the previous example is because $\mu_x$ and $\mu_y$ appear in the different blocks of $A_e$ and never as a product.*

**Example 7.5.** *Consider Problem $P_3$ with homogenous Dirichlet boundary conditions and $f = 1$. In this example the tolerance* tol *is taken as $\varepsilon \times 10^{-3}$.*

For solving the linear system arising from various examples with varying $h$ we employ the nonlinear algebraic multilevel iteration method (NLAMLI), see [7, 8, 19, 20, 23]. The stabilization of the condition number is achieved by using some fixed small number $\nu$ of inner generalized conjugate gradient (GCG) iterations. According to our analysis we choose $\nu = 4$ in all computations. The starting vector for the outer iteration is the zero vector and the stopping criteria is

$$\|r^{(n_{\mathrm{it}})}\|/\|r^{(0)}\| \leq \delta = 10^{-6},$$

where $n_{\mathrm{it}}$ is the number of iterations we report in the tables below. The coarsest mesh in all computations is of size 4×4×4 and has 512 DOF. The finer meshes for $1/h = 8, 16, 32, 64$ consist of $4096, \ldots, 2097152$ DOF, respectively.

TABLE 1. Results for Example 7.1

| $1/h$ | $n_{\mathrm{it}}$ | $\rho$ | sec |
|---|---|---|---|
| 8 | 27 | 0.59 | 0.47 |
| 16 | 27 | 0.60 | 4.76 |
| 32 | 27 | 0.60 | 44.27 |
| 64 | 27 | 0.60 | 422.09 |

TABLE 2. Results for Example 7.2

| | $\varepsilon = 0.1$ | | $\varepsilon = 0.01$ | | $\varepsilon = 0.001$ | |
|---|---|---|---|---|---|---|
| $1/h$ | $n_{\mathrm{it}}$ | $\rho$ | $n_{\mathrm{it}}$ | $\rho$ | $n_{\mathrm{it}}$ | $\rho$ |
| 8 | 25 | 0.57 | 25 | 0.56 | 25 | 0.56 |
| 16 | 28 | 0.61 | 28 | 0.60 | 28 | 0.61 |
| 32 | 30 | 0.62 | 29 | 0.62 | 30 | 0.62 |
| 64 | 30 | 0.62 | 29 | 0.62 | 30 | 0.63 |

First we discuss the results of isotropic problems. In Table 1 we present the number of iterations, the average convergence factor $\rho$ and the total CPU time (including the time for the construction of the preconditioner) for Example 7.1. We observe that the number of iterations is constant and the CPU time is proportional to the problem size which shows that the overall solution process is of optimal order of computational complexity. The same holds for Example 7.2, cf. Table 2. These results also indicate the robustness of the preconditioner with respect to the jumps in the coefficient $\underline{A}$.

Now we discuss the results of anisotropic problems. As we see for Example 7.3 in Table 3 the optimality of our method is still preserved for mild anisotropy, see the column for $\mu_x = 0.1$. However, when the anisotropy gets stronger we observe a small increase in the number of iterations. For the results of Example 7.4 as presented in Table 4, where anisotropy is considered in both $x$ and $y$ directions, we observe a similar small increase in the number of iterations as for Example 7.3. Nevertheless, in this case since the tolerance tol is kept fixed the convergence factor is almost the same for a fixed mesh size $h$ whereas for Example 7.3 the convergence improves since the tolerance is reduced as anisotropy increases. The results of Example 7.5 are presented in Table 5. Here reducing the tolerance

TABLE 3. Results for Example 7.3

| | $\mu_x = 0.1$ | | $\mu_x = 0.01$ | | $\mu_x = 0.001$ | |
|---|---|---|---|---|---|---|
| $1/h$ | $n_{\text{it}}$ | $\rho$ | $n_{\text{it}}$ | $\rho$ | $n_{\text{it}}$ | $\rho$ |
| 8 | 26 | 0.58 | 23 | 0.55 | 22 | 0.53 |
| 16 | 28 | 0.61 | 26 | 0.58 | 24 | 0.56 |
| 32 | 30 | 0.62 | 27 | 0.60 | 25 | 0.57 |
| 64 | 30 | 0.63 | 29 | 0.62 | 27 | 0.59 |

TABLE 4. Results for Example 7.4

| | $\mu_y = 0.1$ | | $\mu_y = 0.01$ | | $\mu_y = 0.001$ | |
|---|---|---|---|---|---|---|
| $1/h$ | $n_{\text{it}}$ | $\rho$ | $n_{\text{it}}$ | $\rho$ | $n_{\text{it}}$ | $\rho$ |
| 8 | 22 | 0.52 | 23 | 0.54 | 22 | 0.52 |
| 16 | 25 | 0.57 | 25 | 0.57 | 25 | 0.57 |
| 32 | 27 | 0.59 | 28 | 0.61 | 28 | 0.60 |
| 64 | 30 | 0.63 | 33 | 0.66 | 30 | 0.63 |

TABLE 5. Results for Example 7.5

| | $\varepsilon = 0.1$ | | $\varepsilon = 0.01$ | | $\varepsilon = 0.001$ | |
|---|---|---|---|---|---|---|
| $1/h$ | $n_{\text{it}}$ | $\rho$ | $n_{\text{it}}$ | $\rho$ | $n_{\text{it}}$ | $\rho$ |
| 8 | 25 | 0.57 | 25 | 0.57 | 25 | 0.57 |
| 16 | 28 | 0.61 | 28 | 0.61 | 29 | 0.61 |
| 32 | 31 | 0.64 | 30 | 0.63 | 33 | 0.66 |
| 64 | 35 | 0.67 | 32 | 0.64 | 37 | 0.68 |

proportionally to $\varepsilon$ did not improve the convergence behavior for a fixed $h$ since apart from the anisotropy in both $x$ and $y$ directions we have the jumps in the coefficients.

We now discuss the task of computing an accurate preconditioner for the pivot block which gets increasingly difficult as anisotropy increases. In Table 6 for Examples 7.1 and 7.3 (with $\mu_x = 0.01$) we report the condition number estimate of the pivot block and its preconditioned matrix for $1/h = 8,\ 16$. We chose these two cases because for Example 7.1 the number of iterations does not vary with the problem size whereas for Example 7.3 the number of iterations slightly increases with the problem size. This also illustrates the effect of adjusting the drop tolerance in ILU(tol) as $\mu_x \to 0$. Unfortunately, taking a very small tol severely affects the sparsity and hence, the overall cost increases. Thus, this is a trade-off between the number of iterations and the cost associated with the ILU factorization and one can not choose an arbitrarily small tolerance. For a comparison see Table 7, where † indicates the increase in computing time as a result of insufficient physical memory.

## 8. CONCLUDING REMARKS

In this paper we generalized our previous work on multilevel preconditioning of systems of linear algebraic equations arising from IP-DG discretization to 3D anisotropic problems. This approach allows for an optimal order solution process. The stabilization

TABLE 6. Growth of condition number of pivot block

| | Example 7.1 | | Example 7.3, $\mu_x = 0.01$ | | |
|---|---|---|---|---|---|
| $1/h$ | $\kappa(A_{11})$ | $\kappa((L_{\text{tol}}U_{\text{tol}})^{-1}A_{11})$ tol $= 1e-02$ | $\kappa(A_{11})$ | $\kappa((L_{\text{tol}}U_{\text{tol}})^{-1}A_{11})$ tol $= 1e-02$ | $\kappa((L_{\text{tol}}U_{\text{tol}})^{-1}A_{11})$ tol $= 1e-04$ |
| 8 | 200.5 | 25.6 | 573.9 | 70.3 | 1.7 |
| 16 | 290.7 | 36.1 | 1762.3 | 218.7 | 6.0 |

TABLE 7. Effect of tol on performance for Example 7.5, $\varepsilon = 0.1$

| | tol $= 1e-03$ | | tol $= 1e-04$ | | tol $= 1e-05$ | | tol $= 1e-06$ | |
|---|---|---|---|---|---|---|---|---|
| $1/h$ | $n_{\text{it}}$ | sec | $n_{\text{it}}$ | sec | $n_{\text{it}}$ | sec | $n_{\text{it}}$ | sec |
| 8 | 29 | 0.60 | 25 | 0.79 | 24 | 1.34 | 22 | 2.81 |
| 16 | 40 | 7.90 | 28 | 9.65 | 26 | 20.18 | 25 | 53.10 |
| 32 | 51 | 88.23 | 31 | 102.09 | 29 | 241.82 | 27 | 722.11 |
| 64 | 66 | 1961.78 | 35 | 1148.82 | 30 | 2560.70 | 27 | 17253.55$^{\dagger}$ |

of the multilevel iteration for 3D problems requires a 4-fold W-cycle whereas in the 2D case the analogous construction of the hierarchical basis required 2-fold W-cycle. Since the coarsening ratio in 3D is 8 (instead of 4 in 2D) this, however, results in approximately the same relative costs with respect to the total number of DOF.

As compared to linear systems obtained from discretization using conforming methods the preconditioning of the pivot ($A_{11}$) block is an even more challenging task since its condition number is proportional to the penalty parameter $\alpha$, which typically grows with recursive applications of the two-level hierarchical basis transformation. Apart from that, the presence of strong anisotropy and large jumps in the coefficients usually deteriorates the quality of an ILU-type preconditioner. This effect is even more severe in case of 3D DG approximations. Future investigations will therefore deal with the construction of highly efficient preconditioners for the pivot block.

## APPENDIX A.

For brevity of the expressions we first introduce the following notations. Let $\delta_x = 2\mu_x - \sqrt{2}\alpha$, $\delta_y = 2\mu_y - \sqrt{2}\alpha$, and $\delta = 2 - \sqrt{2}\alpha$, where $\alpha$ denotes the stabilization parameter of the IP-DG formulation and $\mu_x, \mu_y$ denotes the anisotropy coefficient of the PDE operator in $x$ and $y$ directions respectively. Note that for the isotropic problem, i.e. when $\mu_x = \mu_y = 1$ we have $\delta_x = \delta_y = \delta$. Now, when anisotropy is considered in both $x$ and $y$ directions (normalized with respect to the $z$ direction) the element stiffness matrix $A_e$ has the following structure

$$A_e = \frac{h}{144}\begin{bmatrix} A_{e;\text{int,int}} & A_{e;\text{int,ext}} \\ A_{e;\text{int,ext}}^T & A_{e;\text{ext,ext}} \end{bmatrix}, \tag{30a}$$

where

$$A_{e;\mathrm{int,int}} = \sqrt{2}\begin{bmatrix} 12\alpha & 4\alpha & 4\alpha & \alpha & 4\alpha & \alpha & \alpha & 0 \\ 4\alpha & 12\alpha & \alpha & 4\alpha & \alpha & 4\alpha & 0 & \alpha \\ 4\alpha & \alpha & 12\alpha & 4\alpha & \alpha & 0 & 4\alpha & \alpha \\ \alpha & 4\alpha & 4\alpha & 12\alpha & 0 & \alpha & \alpha & 4\alpha \\ 4\alpha & \alpha & \alpha & 0 & 12\alpha & 4\alpha & 4\alpha & \alpha \\ \alpha & 4\alpha & 0 & \alpha & 4\alpha & 12\alpha & \alpha & 4\alpha \\ \alpha & 0 & 4\alpha & \alpha & 4\alpha & \alpha & 12\alpha & 4\alpha \\ 0 & \alpha & \alpha & 4\alpha & \alpha & 4\alpha & 4\alpha & 12\alpha \end{bmatrix}, \tag{30b}$$

$$A_{e;\mathrm{ext,ext}} = \sqrt{2}\begin{bmatrix} A^F_{e;\mathrm{ext,ext}} & 0 & 0 & 0 & 0 & 0 \\ 0 & A^F_{e;\mathrm{ext,ext}} & 0 & 0 & 0 & 0 \\ 0 & 0 & A^F_{e;\mathrm{ext,ext}} & 0 & 0 & 0 \\ 0 & 0 & 0 & A^F_{e;\mathrm{ext,ext}} & 0 & 0 \\ 0 & 0 & 0 & 0 & A^F_{e;\mathrm{ext,ext}} & 0 \\ 0 & 0 & 0 & 0 & 0 & A^F_{e;\mathrm{ext,ext}} \end{bmatrix}, \tag{30c}$$

$$A^F_{e;\mathrm{ext,ext}} = \begin{bmatrix} 4\alpha & 2\alpha & 2\alpha & \alpha \\ 2\alpha & 4\alpha & \alpha & 2\alpha \\ 2\alpha & \alpha & 4\alpha & 2\alpha \\ \alpha & 2\alpha & 2\alpha & 4\alpha \end{bmatrix}, \tag{30d}$$

$$A_{e;\mathrm{int,ext}} = \begin{bmatrix} A^x_{e;\mathrm{int,ext}} & A^y_{e;\mathrm{int,ext}} & A^z_{e;\mathrm{int,ext}} \end{bmatrix}, \tag{30e}$$

$$A^x_{e;\mathrm{int,ext}} = \begin{bmatrix} 4\delta_x & 2\delta_x & 2\delta_x & \delta_x & -8\mu_x & -4\mu_x & -4\mu_x & -2\mu_x \\ -8\mu_x & -4\mu_x & -4\mu_x & -2\mu_x & 4\delta_x & 2\delta_x & 2\delta_x & \delta_x \\ 2\delta_x & 4\delta_x & \delta_x & 2\delta_x & -4\mu_x & -8\mu_x & -2\mu_x & -4\mu_x \\ -4\mu_x & -8\mu_x & -2\mu_x & -4\mu_x & 2\delta_x & 4\delta_x & \delta_x & 2\delta_x \\ 2\delta_x & \delta_x & 4\delta_x & 2\delta_x & -4\mu_x & -2\mu_x & -8\mu_x & -4\mu_x \\ -4\mu_x & -2\mu_x & -8\mu_x & -4\mu_x & 2\delta_x & \delta_x & 4\delta_x & 2\delta_x \\ \delta_x & 2\delta_x & 2\delta_x & 4\delta_x & -2\mu_x & -4\mu_x & -4\mu_x & -8\mu_x \\ -2\mu_x & -4\mu_x & -4\mu_x & -8\mu_x & \delta_x & 2\delta_x & 2\delta_x & 4\delta_x \end{bmatrix}, \tag{30f}$$

$$A^y_{e;\mathrm{int,ext}} = \begin{bmatrix} 4\delta_y & 2\delta_y & 2\delta_y & \delta_y & -8\mu_y & -4\mu_y & -4\mu_y & -2\mu_y \\ 2\delta_y & 4\delta_y & \delta_y & 2\delta_y & -4\mu_y & -8\mu_y & -2\mu_y & -4\mu_y \\ -8\mu_y & -4\mu_y & -4\mu_y & -2\mu_y & 4\delta_y & 2\delta_y & 2\delta_y & \delta_y \\ -4\mu_y & -8\mu_y & -2\mu_y & -4\mu_y & 2\delta_y & 4\delta_y & \delta_y & 2\delta_y \\ 2\delta_y & \delta_y & 4\delta_y & 2\delta_y & -4\mu_y & -2\mu_y & -8\mu_y & -4\mu_y \\ \delta_y & 2\delta_y & 2\delta_y & 4\delta_y & -2\mu_y & -4\mu_y & -4\mu_y & -8\mu_y \\ -4\mu_y & -2\mu_y & -8\mu_y & -4\mu_y & 2\delta_y & \delta_y & 4\delta_y & 2\delta_y \\ -2\mu_y & -4\mu_y & -4\mu_y & -8\mu_y & \delta_y & 2\delta_y & 2\delta_y & 4\delta_y \end{bmatrix}, \tag{30g}$$

(30h)
$$A^z_{e;\mathrm{int,ext}} = \begin{bmatrix} 4\delta & 2\delta & 2\delta & \delta & -8 & -4 & -4 & -2 \\ 2\delta & 4\delta & \delta & 2\delta & -4 & -8 & -2 & -4 \\ 2\delta & \delta & 4\delta & 2\delta & -4 & -2 & -8 & -4 \\ \delta & 2\delta & 2\delta & 4\delta & -2 & -4 & -4 & -8 \\ -8 & -4 & -4 & -2 & 4\delta & 2\delta & 2\delta & \delta \\ -4 & -8 & -2 & -4 & 2\delta & 4\delta & \delta & 2\delta \\ -4 & -2 & -8 & -4 & 2\delta & \delta & 4\delta & 2\delta \\ -2 & -4 & -4 & -8 & \delta & 2\delta & 2\delta & 4\delta \end{bmatrix}.$$

Moreover, for elements with face(s) $f_s$, $s = 1, \ldots, 6$ lying on $\partial\Omega$ we need to modify these matrices. For brevity reasons again we use the substitutions $\delta^f_x = 4\mu_x - \sqrt{2}\alpha$, $\delta^f_y = 4\mu_y - \sqrt{2}\alpha$, and $\delta^f = 4 - \sqrt{2}\alpha$. Then for a given face $f_s$ on $\partial\Omega$ the matrix $A_{e;\mathrm{int,int}}$ is modified to $A_{e;\mathrm{int,int}} \pm \widetilde{A}_{e;f_s;\mathrm{int,int}}$, where the sign $\pm$ corresponds to the face being on the Dirichlet boundary or the Neumann boundary, respectively, and the correction matrices $\widetilde{A}_{e;f_s;\mathrm{int,int}}$ are given below. Furthermore, for the DOF of the neighboring element we make the respective rows and columns of $A_e$ zero.

(31a)
$$\widetilde{A}_{e;f_1;\mathrm{int,int}} = -\frac{h}{144}\begin{bmatrix} 4\delta^f_x & -8\mu_x & 2\delta^f_x & -4\mu_x & 2\delta^f_x & -4\mu_x & \delta^f_x & -2\mu_x \\ -8\mu_x & 0 & -4\mu_x & 0 & -4\mu_x & 0 & -2\mu_x & 0 \\ 2\delta^f_x & -4\mu_x & 4\delta^f_x & -8\mu_x & \delta^f_x & -2\mu_x & 2\delta^f_x & -4\mu_x \\ -4\mu_x & 0 & -8\mu_x & 0 & -2\mu_x & 0 & -4\mu_x & 0 \\ 2\delta^f_x & -4\mu_x & \delta^f_x & -2\mu_x & 4\delta^f_x & -8\mu_x & 2\delta^f_x & -4\mu_x \\ -4\mu_x & 0 & -2\mu_x & 0 & -8\mu_x & 0 & -4\mu_x & 0 \\ \delta^f_x & -2\mu_x & 2\delta^f_x & -4\mu_x & 2\delta^f_x & -4\mu_x & 4\delta^f_x & -8\mu_x \\ -2\mu_x & 0 & -4\mu_x & 0 & -4\mu_x & 0 & -8\mu_x & 0 \end{bmatrix},$$

(31b)
$$\widetilde{A}_{e;f_2;\mathrm{int,int}} = -\frac{h}{144}\begin{bmatrix} 0 & -8\mu_x & 0 & -4\mu_x & 0 & -4\mu_x & 0 & -2\mu_x \\ -8\mu_x & 4\delta^f_x & -4\mu_x & 2\delta^f_x & -4\mu_x & 2\delta^f_x & -2\mu_x & \delta^f_x \\ 0 & -4\mu_x & 0 & -8\mu_x & 0 & -2\mu_x & 0 & -4\mu_x \\ -4\mu_x & 2\delta^f_x & -8\mu_x & 4\delta^f_x & -2\mu_x & \delta^f_x & -4\mu_x & 2\delta^f_x \\ 0 & -4\mu_x & 0 & -2\mu_x & 0 & -8\mu_x & 0 & -4\mu_x \\ -4\mu_x & 2\delta^f_x & -2\mu_x & \delta^f_x & -8\mu_x & 4\delta^f_x & -4\mu_x & 2\delta^f_x \\ 0 & -2\mu_x & 0 & -4\mu_x & 0 & -4\mu_x & 0 & -8\mu_x \\ -2\mu_x & \delta^f_x & -4\mu_x & 2\delta^f_x & -4\mu_x & 2\delta^f_x & -8\mu_x & 4\delta^f_x \end{bmatrix},$$

(31c)
$$\widetilde{A}_{e;f_3;\mathrm{int,int}} = -\frac{h}{144}\begin{bmatrix} 4\delta^f_y & 2\delta^f_y & -8\mu_y & -4\mu_y & 2\delta^f_y & \delta^f_y & -4\mu_y & -2\mu_y \\ 2\delta^f_y & 4\delta^f_y & -4\mu_y & -8\mu_y & \delta^f_y & 2\delta^f_y & -2\mu_y & -4\mu_y \\ -8\mu_y & -4\mu_y & 0 & 0 & -4\mu_y & -2\mu_y & 0 & 0 \\ -4\mu_y & -8\mu_y & 0 & 0 & -2\mu_y & -4\mu_y & 0 & 0 \\ 2\delta^f_y & \delta^f_y & -4\mu_y & -2\mu_y & 4\delta^f_y & 2\delta^f_y & -8\mu_y & -4\mu_y \\ \delta^f_y & 2\delta^f_y & -2\mu_y & -4\mu_y & 2\delta^f_y & 4\delta^f_y & -4\mu_y & -8\mu_y \\ -4\mu_y & -2\mu_y & 0 & 0 & -8\mu_y & -4\mu_y & 0 & 0 \\ -2\mu_y & -4\mu_y & 0 & 0 & -4\mu_y & -8\mu_y & 0 & 0 \end{bmatrix},$$

(31d)

$$\widetilde{A}_{e;f_4;\mathrm{int},\mathrm{int}} = -\frac{h}{144}\begin{bmatrix} 0 & 0 & -8\mu_y & -4\mu_y & 0 & 0 & -4\mu_y & -2\mu_y \\ 0 & 0 & -4\mu_y & -8\mu_y & 0 & 0 & -2\mu_y & -4\mu_y \\ -8\mu_y & -4\mu_y & 4\delta_y^f & 2\delta_y^f & -4\mu_y & -2\mu_y & 2\delta_y^f & \delta_y^f \\ -4\mu_y & -8\mu_y & 2\delta_y^f & 4\delta_y^f & -2\mu_y & -4\mu_y & \delta_y^f & 2\delta_y^f \\ 0 & 0 & -4\mu_y & -2\mu_y & 0 & 0 & -8\mu_y & -4\mu_y \\ 0 & 0 & -2\mu_y & -4\mu_y & 0 & 0 & -4\mu_y & -8\mu_y \\ -4\mu_y & -2\mu_y & 2\delta_y^f & \delta_y^f & -8\mu_y & -4\mu_y & 4\delta_y^f & 2\delta_y^f \\ -2\mu_y & -4\mu_y & \delta_y^f & 2\delta_y^f & -4\mu_y & -8\mu_y & 2\delta_y^f & 4\delta_y^f \end{bmatrix},$$

(31e)

$$\widetilde{A}_{e;f_5;\mathrm{int},\mathrm{int}} = -\frac{h}{144}\begin{bmatrix} 4\delta^f & 2\delta^f & 2\delta^f & \delta^f & -8 & -4 & -4 & -2 \\ 2\delta^f & 4\delta^f & \delta^f & 2\delta^f & -4 & -8 & -2 & -4 \\ 2\delta^f & \delta^f & 4\delta^f & 2\delta^f & -4 & -2 & -8 & -4 \\ \delta^f & 2\delta^f & 2\delta^f & 4\delta^f & -2 & -4 & -4 & -8 \\ -8 & -4 & -4 & -2 & 0 & 0 & 0 & 0 \\ -4 & -8 & -2 & -4 & 0 & 0 & 0 & 0 \\ -4 & -2 & -8 & -4 & 0 & 0 & 0 & 0 \\ -2 & -4 & -4 & -8 & 0 & 0 & 0 & 0 \end{bmatrix},$$

(31f)

$$\widetilde{A}_{e;f_6;\mathrm{int},\mathrm{int}} = -\frac{h}{144}\begin{bmatrix} 0 & 0 & 0 & 0 & -8 & -4 & -4 & -2 \\ 0 & 0 & 0 & 0 & -4 & -8 & -2 & -4 \\ 0 & 0 & 0 & 0 & -4 & -2 & -8 & -4 \\ 0 & 0 & 0 & 0 & -2 & -4 & -4 & -8 \\ -8 & -4 & -4 & -2 & 4\delta^f & 2\delta^f & 2\delta^f & \delta^f \\ -4 & -8 & -2 & -4 & 2\delta^f & 4\delta^f & \delta^f & 2\delta^f \\ -4 & -2 & -8 & -4 & 2\delta^f & \delta^f & 4\delta^f & 2\delta^f \\ -2 & -4 & -4 & -8 & \delta^f & 2\delta^f & 2\delta^f & 4\delta^f \end{bmatrix}.$$

## Acknowledgments

The authors gratefully acknowledge the support by the Austrian Academy of Sciences.

## References

[1] D. Arnold, An interior penalty finite element method with discontinuous elements, *SIAM J. Numer. Anal.*, 19 (1982), 742–760.

[2] D. Arnold, F. Brezzi, B. Cockburn, and L. D. Marini, Unified analysis of discontinuous Galerkin methods for elliptic problems, *SIAM J. Numer. Anal.*, 39 (2002), 1749–1779.

[3] O. Axelsson, *Iterative solution methods*. Cambridge University Press, 1994.

[4] O. Axelsson and I. Gustafsson, Preconditioning and two-level multigrid methods of arbitrary degree of approximations, *Math. Comp.*, 40(1983), 219–242.

[5] O. Axelsson and P.S. Vassilevski, Algebraic multilevel preconditioning methods I, *Numer. Math.*, 56 (1989), 157–177.

[6] O. Axelsson and P.S. Vassilevski, Algebraic multilevel preconditioning methods II, *SIAM J. Numer. Anal.*, 27 (1990), 1569–1590.

[7] O. Axelsson and P.S. Vassilevski, A black box generalized conjugate gradient solver with linear iterations and variable-step preconditioning, *SIAM J. Matrix. Anal. Appl.*, 12 (1991), 625–644.

[8] O. Axelsson and P.S. Vassilevski, Variable-step multilevel preconditioning methods, I: self-adjoint and positive definite elliptic problems, *Num. Lin. Alg. Appl.*, 1 (1994), 75–101.

[9] R. Blaheta, S. Margenov and M. Neytcheva, Robust optimal multilevel preconditioners for non-conforming finite element systems, *Num. Lin. Alg. Appl.*, 12 (2005), 495–514.

[10] S.C. Brenner and J. Zhao, Convergence of multigrid algorithms for interior penalty methods, *Applied Numerical Analysis and Computational Mathematics*, 2 (2005), 3–18.

[11] F. Brezzi, B. Cockburn, L.D. Marini, and E. Süli. Stabilization mechanisms in discontinuous Galerkin finite element methods. *Report NA-04/24, Oxford University Computing Laboratory*, 2004.
[12] B. Cockburn and C.W. Shu, Runge-Kutta discontinuous Galerkin methods for convection-dominated problems, *Journal of Scientific Computing*, 16(2001), 173–261.
[13] V.A. Dobrev, R.D. Lazarov, P.S. Vassilevski, and L.T. Zikatanov. Two-level preconditioning of discontinuous Galerkin approximations of second order elliptic equations. *Numer. Lin. Alg. Appl.*, 13(2006) 1–18.
[14] J. Douglas Jr., and T. Dupont, *Interior penalty procedures for elliptic and parabolic Galerkin methods, Lecture notes in Phys. 58* Springer-Verlag, Berlin, 1976.
[15] V. Eijkhout and P.S. Vassilevski, The Role of the Strengthened Cauchy-Bunyakowski-Schwarz Inequality in Multilevel Methods, *SIAM Review*, 33(1991), 405–419.
[16] I. Georgiev, J. Kraus, S. Margenov, Multilevel preconditioning of rotated bilinear non-conforming FEM problems, *RICAM-Report 2006-03*, RICAM, Linz, Austria.
[17] J. Gopalkrishnan and G. Kanschat, A multilevel discontinuous Galerkin method. *Numer. Math.*, 95(2003) 527–550.
[18] P.W. Hemker, W. Hoffman, and M.H. van Raalte, Two-level Fourier analysis of a multigrid approach for discontinuous Galerkin discretization, *SIAM J. Sci. Comput.*, 25 (2003), 1018–1041.
[19] J. Kraus, An algebraic preconditioning method for M-matrices: linear versus nonlinear multilevel iteration, *Num. Lin. Alg. Appl.*, 9 (2002), 599–618.
[20] J. Kraus, and S.K. Tomar, Multilevel preconditioning of elliptic problems discretized by a class of discontinuous Galerkin methods, *RICAM Tech. report*, 2006–36.
[21] R. Lazarov, S. Margenov, CBS constants for graph-Laplacians and application to multilevel methods for discontinuous Galerkin systems, *Journal of Complexity*, to appear.
[22] R. Lazarov, P. Vassilevski, L. Zikatanov, Multilevel preconditioning of second order elliptic discontinuous Galerkin problems, Preprint, 2005.
[23] Y. Notay, Robust parameter-free algebraic multilevel preconditioning, *Num. Lin. Alg. Appl.*, 9 (2002), 409–428.
[24] B. Riviere, M.F. Wheeler, and V. Girault, Improved energy estimates for interior penalty, constrained and discontinuous Galerkin methods for elliptic problems I, *Comput. Geosci.*, 3 (1999), 337–360.
[25] Y. Saad, *Iterative Methods for Sparse Linear Systems*, PWS Publishing Company, Boston, 1996.
[26] Ch. Schwab, p- *and* hp- *Finite Element Methods*, Clarendon Press, Oxford, 1998.
[27] K. Shahbazi, An explicit expression for the penalty parameter of the interior penalty method, *Journal of Computational Physics*, 205 (2005), 401–407.
[28] M.F. Wheeler, An elliptic collocation-finite element method with interior penalties, *SIAM J. Numer. Anal.*, 15 (1978), 152–161.

Johann Radon Institute for Computational and Applied Mathematics (RICAM), Austrian Academy of Sciences, Altenbergerstr. 69, A-4040 Linz, Austria

*E-mail address*: {johannes.kraus,satyendra.tomar}@ricam.oeaw.ac.at